Conference Proceedings

EuroSun 2016
Palma de Mallorca (Spain), 11 - 14 October 2016

Linear tube solar receiver as stratified flow vapor generator/separator for absorption machines using $NH_3/LiNO_3$

Antonio Lecuona-Neumann[1], Rubén Ventas-Garzón[1] Ciro Vereda-Ortiz[1] Mathieu Legrand[1]

[1] Dep. Ingeniería Térmica y de Fluidos, Grupo ITEA, Universidad Carlos III de Madrid, Leganés, Madrid (Spain)

Abstract

Straight receiver tubes of either parabolic trough or Fresnel solar collectors can substitute the vapor generator and the solution separator of an absorption machine for producing cold/heat/power, so that no intermediate thermal fluid is required for transporting heat from the collector field to the machine. This way more compact and simpler layouts are possible. Medium temperature solar collectors are attractive for activating innovative cycle absorption machines for producing cold, pumping heat or producing electricity either single or combined.

Solar heat is absorbed directly by the solution that internally slides in the lower segment of an inclined tube by the effect of gravity yielding refrigerant vapor and concentrated solution in a stratified two-phase flow configuration.

The paper in his first part offers an introduction to this innovative technology and I its second part presents a numerical model for the performance evaluation of the concept, highlighting heat transfer issues. Integral 1D steady-state balances are used to establish equations in a simplified form to accelerate pre-design duties and capture main influencing parameters.

Results indicate that this concept is attractive and offers the potential for reducing the cost and burden of nowadays solar facilities in the small and intermediate size range.

Keywords: *Solar cooling, Two-phase flow, receiver tube, parabolic trough, Fresnel, Medium temperature solar collector, stratified flow, direct vapor production.*

1. Introduction

Solar heating and cooling (SHC) concept has been established as a current technology and is well supported by basic studies, such as (Duffie & Beckman, 1980) among others. Recent reviews confirm its interest, e. g. (Mauthner & Weiss, 2013), (The European Technology Platform on Renewable Heating and Cooling, 2014), as well as its potential in different countries has been analyzed, e. g. (CTAER. Solar Concentra., 2015). Nowadays medium temperature (150 – 250 ºC) solar collectors (MTC) e.g. (Jradi & Riffat, 2012) attract much attention because they enable new solar applications for small and medium scale applications. They offer higher flexibility than fixed geometry low-temperature collectors and enjoy the advances in the technology of high-temperature parabolic troughs collectors (HTC) used in large solar power plants.

Solar cooling by a heat pump consumes the solar heat in a thermal machine, generally following an absorption cycle, (Herold, et al., 1996). Some recent studies confirm its interest for industry and for buildings, e. g. (Henning, 2007) (Baniyounes et al., 2013). Typical application is for air conditioning, such as presented in (Henning, 2007), showing a good efficiency of the cycle owing to the mixture Water/Lithium Bromide used as working fluid. Water freezing limits extracting heat below 0 ºC, as water is used as a refrigerant. Ammonia as refrigerant offer the possibility of refrigerating even below -20 ºC and much experience has been accumulated on its use. Ammonia is a natural refrigerant, widely accepted in industry for its reduction capability of greenhouse and ozone depletion gasses (Danfoss, 2015). The absorption cycles using this refrigerant need higher temperatures on the driving source of energy, making medium temperature solar collectors ideal for that.

Currently, ammonia based absorption machines use the mixture Ammonia/Water (Wu et al., 2014). Several studies have performed on-the-field performance evaluation driving the machine with heated fluid through MT solar collectors (Wang, et al., 2015).

doi:10.18086/eurosun.2016.04.11 Available at http://proceedings.ises.org

Ammonia is good for solar energy storage in combination with absorbents, either solid or liquid, e. g. (Yu, et al., 2013), enhancing its interest in SHC.

Machines using Ammonia/Water need a rectification tower to purify the ammonia vapor reducing minute proportions of water. The solution of Ammonia into Lithium Nitrate salt ($NH_3/LiNO_3$) offers to eliminate this bulky and expensive component, but salt crystallization at the inlet of the absorber must be avoided. This solution offers a lower risk of corrosion than Ammonia/Water. Several studies confirm the potential of this working fluid (Ventas et al., 2010). Some operating test results are available (Hernández-Magallanes, et al., 2014). Even pre-industrial prototypes are now operative (Zamora et al., 2014).

The current layout of a solar cooling facility includes an outdoor primary circuit of a heat transfer fluid (HTF) including anti-freeze capability, a secondary indoor circuit, typically of water, including a heat storage tank and a tertiary circuit of cold water, (Kalogirou S. , 2004) (Lecuona et al., 2009). A heat rejection circuit is also needed when the machine is not air cooled. This leads to a high complexity and high procurement, high maintenance costs and the need of professionals for this. The end result is an increase in the Levelized Cost of Energy (LCOE). In addition, there appears some reluctance to invest, reinforced by the tailored character of every facility. Some studies confirm this appreciation, e. g. "*The lack of an optimized solution is the most critical barrier for rural or off-grid application of CSP*", in (The Carbon Thrust, 2013). Meaning "CSP" Concentrated Solar Power.

Direct steam production is an objective in large solar power plants, e.g. (Eck, et al., 2003) and (Kalogirou et al., 1997) always underpinning the objective of simplification, cost reduction, and higher energy efficiency. In solar cooling facilities, this can also be explored. The working fluid of the absorption machine has to flow partially filling the solar collector receiver tube, this way simplifying the facility and drastically eliminating the cost of heat exchangers, piping, and HTFs. In absorption machines, the liquid phase evaporates only some % of mass. This precludes the dangerous dry-out and rewetting processes. Refrigerant vapor separation is not needed at the outlet as it happens spontaneously thanks to the density difference. Stratified flow favors this, as the liquid phase flows falling under gravity effect in the lower part of an inclined tube, while the vapor phase flows upwards in the opposite direction, already separated, see Fig. 1 as it is progressively heated by the wall. This layout allows reducing the tube peripheral temperature gradients in Fresnel collectors and in parabolic trough ones near midday (Lecuona-Neumann et al., 2016).

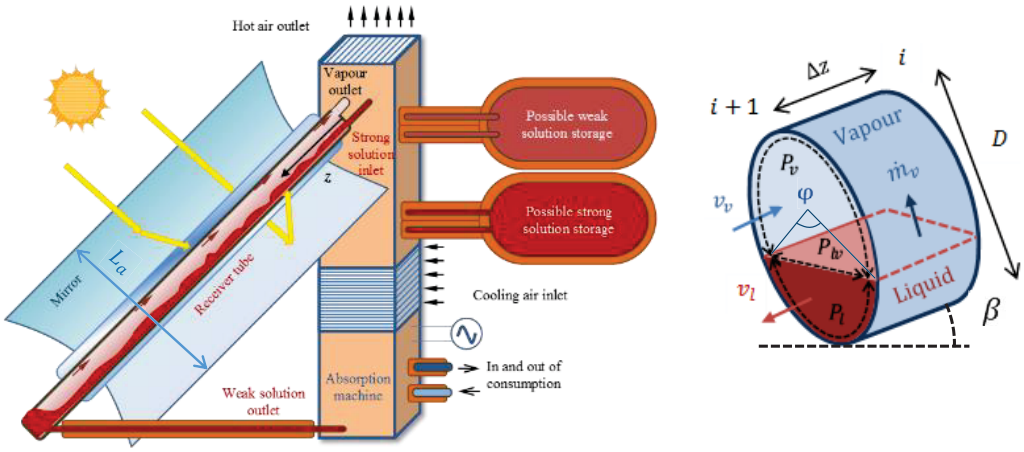

Fig. 1: Left: Scheme of an elementary solar cooling layout with gravity stratified flow in the receiver tube and attached air cooled absorption machine, eventually incorporating energy storage. Right: 1D flow discrete element.

The proposed layout is shown in Fig. 1. It includes an air-cooled absorption machine attached to the solar collector ensemble. This way no indoor building space is consumed for the machine room. Freezing/crystallization of the $NH_3/LiNO_3$ solution is no problem down to around -15 ºC ambient temperature with no specific measures.

The higher driving temperature with MTCs allows the application of advanced cycles (Ventas et al., 2016). This way several opportunities appear to reduce the Levelized Cost of Energy (LCOE) and increase coverage of the user demand: i) cooling capacity boost consuming electricity with the same machine (Vereda et al., 2014),

ii) directly produced or pumped heat production in winter, iii) increased COP using double stage/double effect (Ventas et al., 2016) and iv) even allowing electricity production in periods when neither heat nor cold is needed. NH_3 is suitable for this purpose as it generates high-pressure differentials between condenser and evaporator, allowing expanders to produce work. Small scale MT solar collectors can be built with stationary receiver tubes, thus eliminating the extra cost to avoid NH_3 leaks that are typical in large format high-temperature parabolic trough solar collectors that use articulated tubing.

This paper addresses the basic analysis of the vertically stratified flow using a simplified 1D modeling of the solar collector receiver tube of a circular cross-section, following a sequential calculation process. Stratified flow is assumed. The low velocities involved precludes either annular flow or appreciable effect of waves on the free surface of the liquid, excepting an effective roughness increase, as the inclination of the receiver tube ranges from several degrees up to the local latitude plus solar declination (Wallis, 1969). Application of the model to the promising mixture $NH_3/LiNO_3$ is performed and consequences are obtained aiming at pre-design and optimization duties.

2. Numerical model assumptions

The stratified or wavy-stratified nature of the flow is supported by the moderate mass flux and the relatively high void fraction in the flow, according to (Turgut et al., 2016) among others. Here the liquid phase is gravity driven, such as in (Faccini et al., 2015). Even this, here both flows are counter-current, differently to the most analyzed layout of co-current pressure driven two-phase flow inside typically small diameter tubes, e. g. (Issa R. I., 1988).

The slenderness of the receiver tube(s) of a parabolic trough or Fresnel type solar collector facilitates 1D modeling as a separated stratified flow with no liquid holdup, allowing separate equations and flow variables for both flows (Wallis, 1969). There the full set of governing equations applicable to the opposite direction flows is described in a generic way, as well as the single interphase jump conditions. One difficulty in the proposed layout is that the single outlet of the vapor flow is the accumulation of the opposite liquid flow vapor production and heat transfer, both with the tube wall and the interphase. In addition to that, there is mutual friction at the interphase free surface with the added complication of evaporation. This coupling makes necessary solving a large number of simultaneous equations for balances, fluid properties, and momentum plus heat transfer, when applied to a discrete number of finite elements of the tube along z, Fig.1. This would mean around 10 to 15 equations per element. Momentum and heat balances are not a closed issue when establishing 1D equations across a surface where there is evaporation because the 1D flow is represented by a single average velocity, density, temperature and NH_3 mass fraction. Some issues can be found in (Wallis, 1969) and a complete treatment is presented in (Issa, 1988) for co-current laminar (Ullmann et al., 2004) and turbulent flow with wavy interphase (Ullmann & Brauner, 2006). Fortunately, heat and momentum transfer to the liquid from the vapor flow can be considered negligible without much loss in accuracy for our case, as is supported below.

1D governing equations are coherent with heat and mass transfer correlations for respectively Sherwood and Nusselt numbers, especially when both concentrations and temperatures can safely be averaged in a cross section.

Nusselt number Nu for the liquid and vapour flow are of the same order of magnitude, as well as hydraulic diameters and wall contact areas, but for extreme cases. Thermal conductivity of NH_3 vapour is one to two orders of magnitude less than that of the liquid solution, yielding the heat transfer coefficients in the same proportion. Thus heat transfer from vapour to liquid $\dot{q}_{vl}$ can be considered negligible in front of wall-to-liquid heat transfer rate $\dot{q}_{wl}$. In addition to that the smaller heat capacity of NH_3 makes this flow approaching the wall average temperature $T_w\langle z\rangle$ faster than the liquid, so that $\dot{q}_{wl} \gg \dot{q}_{wv}$. From now on $\langle\ \ \rangle$ means functional dependence. As a consequence the net absorbed, solar heat will be applied only to the liquid as a first approximation.

Friction stress across the interphase is continuous. At the indicated pressure ~ 15 bar one finds $\rho_l \sim 10^2 \rho_v$, the vapor production is about Δx =3-8% in mass. The chosen void fraction $\alpha = A_v/A_l$ is large to minimize ammonia inventory for safety reasons. This makes $v_v \sim v_l$ by mass conservation; actually at the liquid outlet $v_v = 0$ and at the vapor outlet $v_v = \frac{\Delta x}{1-x}\frac{\rho_l}{\rho_v}\frac{v_l}{\alpha}$, see Fig. 2 to 5. This is in contrast with the much studied two-phase co-current flow in evaporators and boilers, whose mission is oriented toward either the full or a substantial phase change, implying significant acceleration near the shared outlet, with the frequent result of

liquid hold up. Friction factors $f_l \sim f_v$ as Reynolds numbers are of the same order of magnitude, mainly owing to the much larger hydraulic diameter of the vapor flow on which they are based, $Re_l \sim Re_v \rightarrow \frac{1}{2}\rho_l(v_l - v_{lv})^2 f_l = \frac{1}{2}\rho_v(v_l + v_{lv})^2 f_v$, the velocity of the interphase v_{lv} is near the liquid velocity v_l. For the case indicated in Fig. 2, at $z = 0$ $Re_l = 3{,}8 \times 10^3$ and $Re_v = 4{,}6 \times 10^3$. In This means that the liquid surface can be considered free of viscous stress with not much loss in accuracy. According to this, the pressure loss of the vapour flow is negligible in front of the tube pressure, which is determined by the saturation pressure of pure ammonia in the condenser of the absorption machine $p_s\langle T_c\rangle$, in the order of 5-20 bar when T_c is atmospheric temperature plus 5 to 10 K. Only needing standard commercial information of the collector is another advantage of this approach.

Similar reasoning will lead to considering limiting the heat transfer coefficient α_v in the mutual heat transfer at the interphase.

According to (Cussler, 2009) p. 504, mass diffusion relaxation time τ in turbulent flows is controlled by the summation of two mutually independent relaxation times, the first one is for the formation of packets of size l and the second one is for molecular diffusion into these packets with coefficient D_{diff}; this datum is obtained from (Infante-Ferreira, 1985). This leads to total a relaxation length L_τ:

$$\left.\begin{array}{r} \tau = \frac{D^2}{4E} + \frac{l^2}{4D_{diff}};\ L_\tau = v_l\tau \\ Pe = \frac{Dv_l}{E} = 2 \\ v_l \approx 2\frac{\mathrm{m}}{\mathrm{s}};\ D \approx 5\ \mathrm{cm} \\ l{\sim}30\ \mu\mathrm{m};\ D_{diff}{\sim}10^{-5}\frac{\mathrm{cm}^2}{\mathrm{s}} \end{array}\right\} \rightarrow E \approx 500\frac{\mathrm{cm}^2}{\mathrm{s}} \Bigg\} \rightarrow L_\tau = \left(\frac{D^2}{4E} + \frac{l^2}{4D_{diff}}\right) = (0{,}013\ \mathrm{s} + 0{,}2\ \mathrm{s})2\frac{\mathrm{m}}{\mathrm{s}} = 0{,}4\ \mathrm{m} \qquad \text{(eq.1)}$$

With collector length of 4-20 m this indicates that assuming negligible transversal concentration gradients in the liquid bulk is assumable, thus saturation can be accepted at the vapor pressure as a first approximation. Pure NH_3 forms the vapor flow, thus the mass diffusion resistance is null for this vapor flow. For temperature through the interphase, a jump is accepted between both well-mixed vapor and liquid flows as a reasonable assumption, in the turbulent regime for the resultant Reynolds numbers Re. No hydraulic pressure is considered in the liquid.

As a consequence, and in order to develop a comprehensive model, the simplifying assumptions are steady state and well mixed fully developed flows, flat free interphase with a rough surface owing to low amplitude waves, saturation equilibrium at the adiabatic interphase for liquid flow, but diabatic for vapor flow at constant pressure. Radiation and buoyancy are negligible effects inside the tube. Friction of the gas phase is negligible for the liquid flow. Constant liquid central angle φ ($\varphi = \pi$ for diameter) derives into constant falling velocity v_l $\forall z \in [0, L]$. Constant wall temperature T_w is assumed around the tube periphery, but variable along z. Solar radiance is constant along z.

Comprehensive models have been developed for the local efficiency of the parabolic trough solar collector and the subsidiary calculation of the tube wall temperature, e. g. (Forristal, 2003). For the lower optical concentration that MTCs have in comparison with HTCs and for liquid flow, the temperature average difference between wall $\overline{T}_w$ and fluid $\overline{T}$ is small, in the order of 20 ºC. This allows using the local average wall temperature instead of the fluid temperature averaged from inlet to outlet, not hindering the accuracy of the model. On the other hand this reduces the computing load substantially and allows to use available commercial information in solar collector performance. For simplicity it is acceptable using the reduced characteristic efficiency equation (no wind, no axial incidence, steady-state) determined according to standards such a (ISO/DIS 9806, 2016). As the characteristic curve is quite horizontal at the usual values of T not compromising error is expected. This curve is reduced to:

$$\eta\langle T_w\rangle = a_0 - \frac{a_1(T_w - T_{amb}) - a_2(T_w - T_{amb})^2}{G_{Tb}} \qquad \text{(eq.2)}$$

G_{Tb} is the tilted beam irradiance.

3. Numerical model setup

Terminal liquid velocity is assumed to happen just at the inlet. As a consequence average falling velocity

derives from the balance between gravity and wall friction, resumed into a Darcy friction factor $f_{D_{h,l}}$, function of the liquid hydraulic diameter through the liquid flow Reynolds number Re_l and the relative roughness of the wall $\varepsilon_r = \varepsilon/D_h$, where ε is the absolute equivalent roughness.

$$v_l^2 = \frac{2g\sin(\beta)D_{hl}\langle\varphi\rangle}{f_{D_{hl}}\langle Re_l,\epsilon_r\rangle};\ D_{hl}\langle\varphi\rangle = \frac{4A_l\langle\varphi\rangle}{P_l\langle\varphi\rangle};\ A_l\langle\varphi\rangle = \frac{D^2}{8}(\varphi - \sin\varphi);\ P_l\langle\varphi\rangle = \frac{D}{2}\varphi\ ; Re_l = \frac{4\dot{m}_l}{\mu_l\langle x,T\rangle D_{hl}} \quad \text{(eq.3)}$$

This expression neglects the momentum transfer by evaporation (Wallis, 1969), negligible in our case. This is an approximation that fits well into other analytical approximations, such as (Hetsroni, 1982) p. 2-84, originally by (Taitel & Dukler, 1976), although that considers the coflowing configuration. An implicit continuity equation allows solving for liquid central angle $\varphi\ \forall z\ \epsilon\ [0, L]$ for a given liquid mass flow $\dot{m}_l$, applied to the inlet ($_{in}$):

$$\rho_l\langle x_{in}, T_{in}\rangle v_l A_l\langle\varphi\rangle = \dot{m}_l \quad \text{(eq.4)}$$

The liquid density ρ_l is function of the local NH_3 mass fraction x and liquid temperature T. At the liquid inlet $z = 0$ ($_{in}$) pressure p is equal to the saturation of pure ammonia at the machine condenser $p_{s,NH_3}\langle T_c\rangle$. At the same point we consider, saturated inlet of the liquid solution. Subcooled or superheated solution is not considered here. Constancy of pressure both across the interphase and along z in addition to the saturation condition allow determining the NH_3 mass fraction x at any axial location z, including the outlet $z = L$ ($_{ou}$), $i = n$ when T were determined for any z:

$$p_l\langle x_{in}, T_{in}\rangle = p_l\langle x_{ou}, T_{ou}\rangle = p_l\langle x, T\rangle = p_{s,NH_3}\langle T_c\rangle \doteq p \quad \text{(eq.5)}$$

The machine condensation temperature T_c is the ambient temperature T_{amb} plus 5º to 10 ºC, depending on the heat rejection parameters. This assumption neglects the pressure decrease towards $z = 0$ because of friction and gravity and also because of the accelerating vapour flow that appears as a consequence of the accumulation of evaporation from $z = L$ down to $z = 0$. Its order of magnitude is $\rho_v v_v \frac{\partial v_v}{\partial z} L \sim \rho_v \left[\frac{(x_{in}-x_{ou})\dot{m}_l}{\rho_v A_v}\right]^2$, negligible in front of p.

As a consequence of constant pressure and saturation both x and T for the liquid are related this way:

$$\mathrm{d}p\langle x, T\rangle = 0 = \frac{\partial p}{\partial x}\mathrm{d}x + \frac{\partial p}{\partial T}\mathrm{d}T \rightarrow \frac{\mathrm{d}x}{\mathrm{d}T} \doteq x_T\langle x, T\rangle = -\frac{\partial p}{\partial T}\Big/\frac{\partial p}{\partial x} \quad \text{(eq.6)}$$

Only transversal heat transfer is considered, neglecting it in the z direction. Wall temperature tangential and radial gradients are considered negligible. Wall temperature T_w can be determined along z assuming that all the absorbed heat is transferred to the liquid, through a heat balance, where the heat transfer coefficient is α_{wl} and the aperture width of the mirror is L_{ap} (Fig. 1) on which a beam irradiance G_{Tb} is normal:

$$T_w = T_{amb} + \frac{\left(b^2+4a\right)^{0.5}-b}{2}\ ;\ a = (T - T_{amb})c + \frac{G_{Tb}a_o}{a_2};\ b = \frac{a_1}{a_2} + c\ ;\ c = \frac{P_{tl}\alpha_{wl}}{a_2 L_{ap}}\ ;\ P_{tl} = P_l \quad \text{(eq.7)}$$

For the local heat transfer coefficient α, either for liquid or vapour flow, a Gnielinski correlation (Gnielinski, 1976) has been chosen for the Nusselt number Nu in the turbulent regime ($2{,}300 < Re_{D_h}$) including the Prandtl number $Pr = c_p\mu/k$ and the friction factor from (Haaland, 1983) ($4{,}000 < Re_{D_h}$). Correction for the entrance region has been chosen from (Al-Arabi, 1982), referred in (Sigalés, 2003) p. 645. Correction for vapor transpiration at the interphase is neglected.

$$\alpha = Nu\frac{k}{D_h};\ Nu = \frac{\frac{f}{8}\left(Re_{D_h}-1000\right)Pr}{1+12.7\left(\frac{f}{8}\right)^{\frac{1}{2}}\left(Pr^{\ 2/3}-1\right)}\underbrace{\left(1 + 2.8(1-0.8)\left(\frac{D}{z}\right)^{0.8}\right)}_{C_{en}};\ f = -1.8\log\left(\left(\frac{\epsilon_r}{3}\right)^{1.11} + \frac{6.9}{Re_{D_h}}\right) \quad \text{(eq.8)}$$

The entry length correction C_{en} is for local Nu, here considered on the high side of the several formulae found in the literature, but not the highest. No correction has been implemented in α_{lv} because of vapour blowing out of the liquid free surface ($\dot{m}_v$) as it is of low magnitude (Sigalés, 2003).

The explicit (eq.4) allows calculating T progressively from inlet to outlet through the net solar heat received by a finite element Δz, between control surfaces i and $i + 1$. Using an Euler explicit advancing scheme this leads to:

$$T_{i+1} = T_i + \frac{L_{ap} G_{Tb} \eta \langle T_w \rangle}{\dot{m}_{l,i}(c_l - c_x)_i} \Delta z \; ; c_x = x_T \frac{\partial h}{\partial x} ; T_0 = T_{in} \quad \text{(eq.9)}$$

$c_x < 0$ takes into account the evaporation, acting as an increased effective specific heat c_l for the liquid. The increase in temperature leads to a decrease in x and the corresponding production of vapour at each element $\dot{m}_v$:

$$x_{i+1} = x_i + x_T(T_{i+1} - T_i) \; ; z = L \; \rightarrow x_{ou} = x_n \quad \text{(eq.10)}$$

In order to check the validity of assuming constant φ and v_l, local liquid mass flow can be corrected by:

$$\dot{m}_{l,i+1} = \dot{m}_{l,i} - \dot{m}_{v,i+1} \quad \text{(eq.11)}$$

And verify that the loss in mass can be just up to around 3%-8% along L. The accumulated vapour at point i can be calculated afterwards. The vapour velocity could be calculated when its temperature T_v is previously calculated:

$$\dot{m}_{av,i} = \sum_{j=n}^{j=i} \dot{m}_{v,j} \; ; \; n = \frac{L}{\Delta z} \; ; v_v = \frac{\dot{m}_{av,i}}{\rho_v \langle p, T_v \rangle} \quad \text{(eq.12)}$$

T_v at station i, is the result of mixing from $j = n$ down to $j = i$ and the cumulative heating from the walls and free surface of the liquid. Both of them must result in a negligible figure in front of the heat transferred from walls to the liquid for the simplifying assumptions to be valid. Assuming an average $c_{p,v}$ in the mixing process:

$$T_{v,i-1} = \frac{\dot{m}_{v,i} T_{v,i} + \frac{\left[\alpha_{wv,i}\left(T_{w,i} - T_{v,i}\right) P_v + \alpha_{v,i}\left(T_i - T_{v,i}\right) P_{lv}\right]}{c_{pv,i}}}{\dot{m}_{av,i} + \dot{m}_{v,i}} \; ; T_{v,n} = T_n \quad \text{(eq.13)}$$

4. Fluid properties

Ammonia properties are evaluated using the FluidMAT® software (Kretzschmar, Stoecker, Kunick, & Blaeser, 2015), mainly based on Tillner-Roth formulation (Tillner–Roth et al., 1993).

Ammonia/Lithium Nitrate solution properties are not so well documented. The properties of (Libotean et al., 2007) and (Libotean, et al., 2008) were used, extended for lower ammonia mass fraction and higher temperatures from data of the same source, still to be published. These results were checked against (Farshi et al., 2014) for enthalpy, correcting the reference datum. Thermal conductivity was obtained from (Cuenca et al., 2014). Crystallization boundary data, originally from (Infante Ferreira, 1984) were reported in (Wu et al., 2013). The adaptation was performed to formulate the boundary line in a more convenient form for the model.

5. Results

First, some characteristic data are presented and then a parametric study shows the results. Maximum representative irradiance has been taken into account $G_{Tb} = 800$ W m^{-2}, no wind and steady-state operation with an ambient temperature $T_{amb} = 30$ ºC.

The model can be applied to a representative MTC, in this case, the Abengoa PT-1 small scale MTC, shown in Tab. 1 (Solar Rating & Certification Corp., 2014).

Tab. 1: Basic data for the representative concentrating MTC Abengoa-IST PT-1. Effects of wind, sky infrared radiation and incidence are ignored. * for reported net aperture surface.

L_{ap} * [m]	L * [m]	$a_0 \equiv F'(\tau\alpha)_{en}$ [-]	a_1 [W m^{-2}K^{-1}]	a_2 [W m^{-2} K^{-2}]	Original fluid	T_{max} allowed [ºC]
2.2	6.0	0.71	0.3581	0.0019	water	250

For the inlet conditions, the condenser temperature chosen is $T_c = T_{amb} + 10$ K. This corresponds to $p = 15.5$ bar. Choosing an inlet temperature $T_{in} = 100$ ºC this corresponds to $x_{in} = 0.428$, thus no subcooling is considered in this case, neither the presence of bubbles at the inlet. A large inclination angle $\beta = 40$ º will be near optimum for capturing sun rays at mid-latitudes, for a collector oriented toward the equator, e. g. Madrid (Spain). $G_b = 800$ W m^{-2}, this is a compromise between the highest expected with the adequate collector inclination β around noon during a clear day and tracking the sun with a single axis, around 1.000 W m^{-2}, and an average figure because of some longitudinal incidence and cloudiness.

The flow evolution for this case is shown in Fig. 2 with some extra data indicated in the caption. It is worth to highlight:

- The evolution of the flow variables is linear, excepting wall and to a lower extent vapor temperatures. This is a consequence of the increase of α_l; α_v and α_{lv} in the entry region, around 0.5 to 1.0 m. Eliminating this correction in α (eq.8) eliminates these non-linearities. This would occur in a second additional collector located downstream the first one, Fig. 3.
- The downstream increase of T_w, does not substantially affect the local efficiency of the collector η, owing to its high stagnation temperature. This supports using the characteristic efficiency curve with T_w (eq. 2) instead of calculating the collector heat losses. The resulting average efficiency is $\eta_{av} = 0.64$.
- T_l increases up to 136 ºC in this case. This implies: a) a lower rate of the decrease downstream (decrease along z) of the vapor temperature T_v, as it is the result of mixing of vapor produced upstream b) wall heating near the exit and cooling near the inlet c) liquid cooling all along. In order to indicate the proportion of cooling by the liquid, $T_{v,a}$ indicates exclusion of any heat transfer. $T_{v,ou} = 117$ º; $T_{va,ou} = 115$ ºC. These temperatures are higher than the liquid inlet wall temperature at the same station, $T_{w,in} = 109$ ºC.
- There is a fairly constant difference between wall and liquid temperatures downstream the entrance region, 9 ºC at the inlet and around 15 ºC downstream the entrance length.
- $x_{ou} = 0.344$, meaning an 8.41% decrease from the inlet. This means a crystallization temperature of 15 ºC.

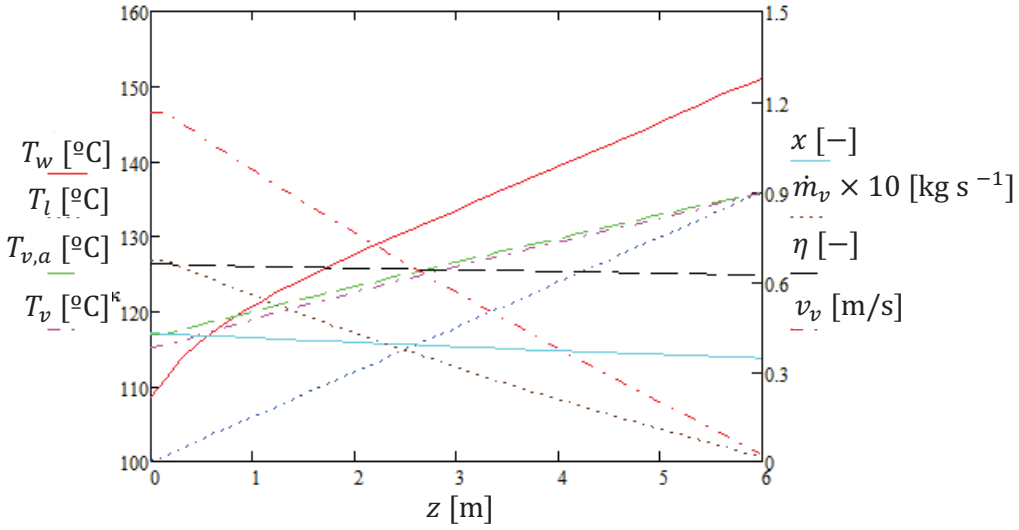

Fig. 2: Evolution along z of flow variables with $L = 6$ m; $D = 3$ cm; $m_l = 0.0833$ kg s^{-1}; $\beta = 40$ º; $\varepsilon = 0.1$ mm; $\varphi = 90$ º; $v_l = 1.32 \frac{\mathrm{m}}{\mathrm{s}}$.

One interesting question is how the length of the collector L affects the performance for constant mass flow. Fig. 3 uses the same input condition than Fig. 2 (ceteris paribus) but doubles the length of the collector, $L = 12$ m. The cooling of the vapour now is, $T_{v,a} - T_v = 6$ ºC. $x_{ou} = 0.28$, resulting in a crystallization temperature of 47 ºC, thus impeding operation of the absorption machine unless mass flow rate is increased. This is the logical choice as the solar power will be around twice. Fig. 4 shows the results of doubling the mass flow ceteris paribus; $x_{ou} = 0.343$.

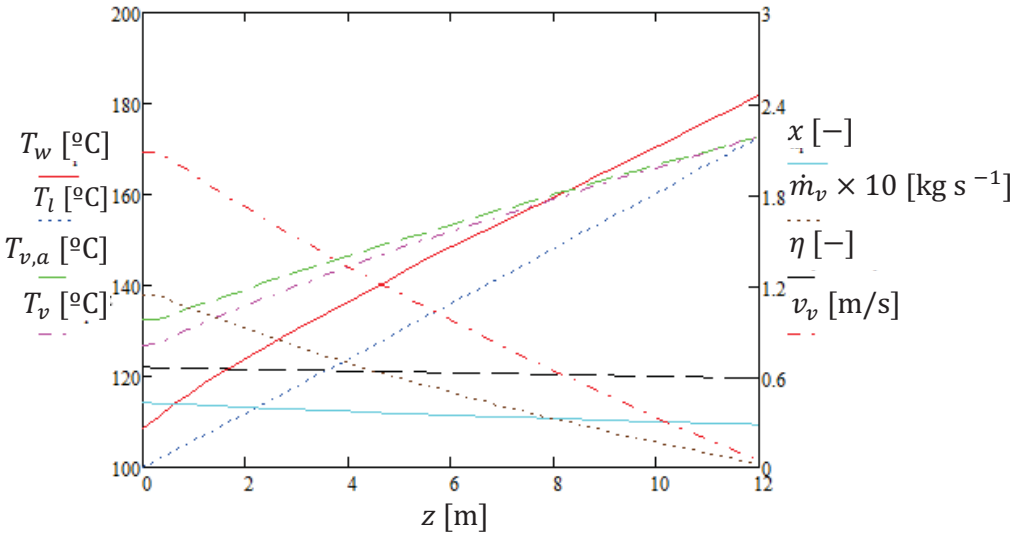

Fig. 3: Evolution along z of flow variables with $L = 12$ m $D = 3$ cm; $m_l = 0.0833$ kg s^{-1}; $\beta = 40$ º; $\varepsilon = 0.1$ mm; $\varphi = 90$ º; $v_l = 1.32 \frac{\text{m}}{\text{s}}$.

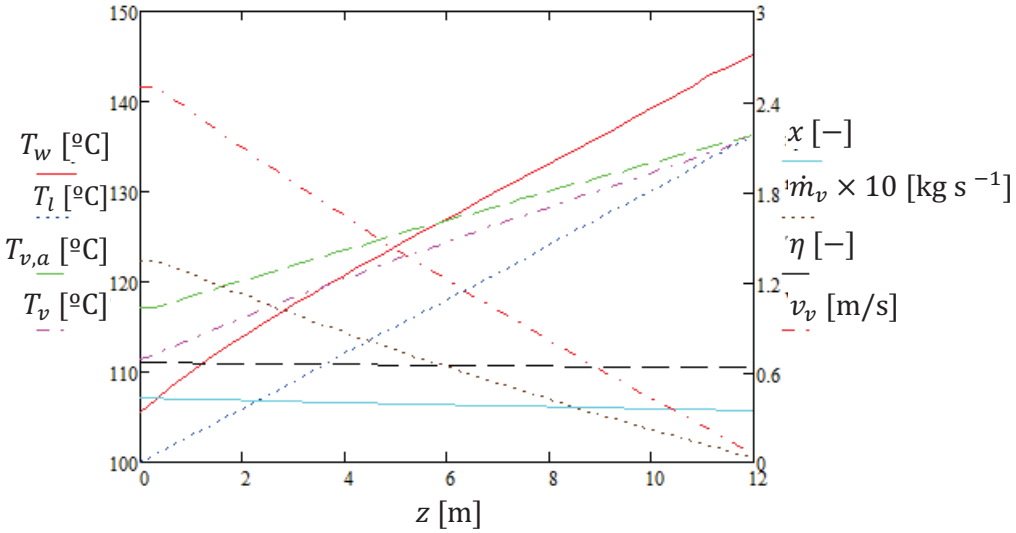

Fig. 4: Evolution along z of flow variables with $L = 12$ m $D = 3$ cm; $m_l = 0.167$ kg s^{-1}; $\beta = 40$ º; $\varepsilon = 0.1$ mm; $\varphi = 108$ º; $v_l = 1.61 \frac{\text{m}}{\text{s}}$.

The possibility of selecting different inclination facilitates the installation in different ceiling surfaces of buildings. Thus the effect of changing inclination angle β is interesting. Fig. 5 shows decreasing down to 5 º. This is valid for equatorial locations with the same G_b, but lower values should be expected at higher latitudes. The result is partially similar to the ones presented in Fig. 2, $x_{ou} = 0.344$; this means the same vapour production with the 40 º inclination, ceteris paribus, but the wall temperature is higher, although not affecting η. This is an interesting results as it indicates that the inclination angle can be widely changed. Now vapor suffers a small net heating.

Simplifying hypothesis now do not hold so well owing to the increased φ implying an increase in depth of the liquid vein that would limit reaching near NH_3 equilibrium in the bulk liquid flow. The lowest Reynolds number is for this case, $Re_l = 3{,}780$.

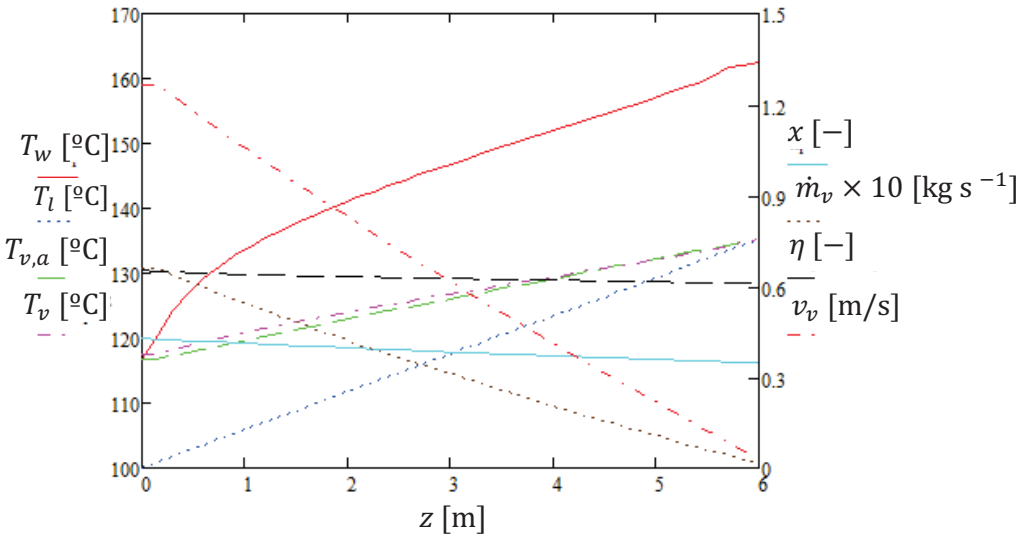

Fig. 5: Evolution along z of flow variables with $L = 6$ m; $D = 3$ cm; $m_l = 0.0833$ kg s^{-1}; $\beta = 5$ º; $\varepsilon = 0.1$ mm; $\varphi = 116$ º; $v_l = 0.67 \frac{\mathrm{m}}{s}$.

6. Conclusions and further work

Reasonable simplifications lead to the development a comprehensive 1D model of the flow evolution along the receiver tube of a parabolic trough solar collector under separated stratified two-phase flow. This model allows a sequential calculation that almost avoids iterations, excepting the liquid angle φ single equation calculation. The results support the simplifying assumptions. The model emphasizes the heat transfer process under evaporation in a MT solar collector.

The moderate heat flux from wall to liquid, always below 10 kW/m^2, the large interphase surface and temperature differences between the wall and liquid smaller than 5 K allow to be confident on the absence of significant bubble formation, thus nucleate boiling does not have to be taken into account excepting the lowest inclination angle, such as $\beta = 5$ º, Fig. 4 (Ghoshhdastidar, 2004). This large temperature difference, in spite of the low heat flux, is due to the small heat conductivity of the solution $k_l \approx 0.3$ W m^{-1}K^{-1} in comparison to water.

The innovative operation of a solar collector here described is meant for its application as a vapor generator and separator of an integral absorption machine using the promising solution $NH_3/LiNO_3$. This allows cold production at subzero temperatures using medium temperatures of the driving heat in the range of 100-200 ºC. This working fluid allows other possibilities, such as COP larger than 1.0 if double effect is used, electric backup if a hybrid cycle (Vereda, et al., 2014) is used and presumably electricity production using an expander in the refrigerant branch of the cycle.

The counter-flow layout allows minimizing heating of the vapor, owing to the cooling effect by the liquid and also by the wall near the liquid inlet. This is favorable for the operation of the absorption machine as a chiller, reducing the load of the condenser and increasing the collector efficiency. For producing power an alternative coflowing layout would be favorable because the higher is the vapor temperature the higher is the enthalpy at the inlet of the expander. Thus the enthalpy jump is higher.

Further work will likely include the effects of the mass transfer resistance in the liquid and the non-uniform transversal temperature in the tube wall, using newly developed simplified calculus (Lecuona-Neumann et al., 2016). Another line of work would be to study the evolution when the solution enters the tube subcooled or superheated. The inclusion of some correction for the interphase heat transfer in eq. 9 will increase the accuracy of the model. Experimental validation is under work.

7. Acknowledgements

The partial funding of the research project “Tecnologías energéticas térmico-solares y de aprovechamiento de calores residuales a baja y media temperatura integradas en la red eléctrica”, ENE2013-45015-R from the

Spanish Ministerio de Economía y Competitividad is greatly appreciated.

8. References

Al-Arabi, M.,1982. Turbulent Heat Transfer in the Entrance Region of a Tube. *Heat Transfer Engineering, 3*(3), 76-83. doi:10.1080/01457638108939586.

Baniyounes, A. M., Ghadi, Y. Y., Rasul, M. G., & Khan, M., 2013. An overview of solar assisted air conditioning in Queensland's subtropical regions, Australia. *Renewable and Sustainable Energy Reviews, 26*, 781–804. doi:10.1016/j.rser.2013.05.053.

CTAER. Solar Concentra., 2015. *Mercado Potencial En España y Aplicaciones en Tecnologías Solares de Concentración de Media Temperatura. Informe económico.* Sevilla, Spain: CTAER.

Cuenca, Y., Salavera, D., Vernet, A., Teja, A., & Vallés, M., 2014. Thermal conductivity of ammonia+lithium nitrate and ammonia+lithium nitrate+water solutions over a wide range of concentrations and temperatures. *International Journal of Refrigeration, 38*, 333–340. doi:10.1016/j.ijrefrig.2013.08.010.

Cussler, E., 2009. *Diffusion Mass Transfer in Fluid Systems 3rd ed.* Cambridge, UK: Cambridge University Press.

Danfoss., 2015. *De los HFC/HCFC al amoníaco en la refrigeración industrial. Una guía breve sobre el cambio al amoníaco.* Danfoss Group Global. Copenhaguen: Danfoss A/S. Retrieved November 11, 2015, from www.danfoss.com/IR-tools.

Duffie, J., & Beckman, W., 1980. *Solar Engineering of Thermal Processes 3rd ed.* Hoboken, New Jersey, USA: Wiley.

Eck, M., Steinmann, W.-D., & Rheinländer, J., 2004. Maximum temperature diff erence in horizontal and tilted absorber pipes with direct steam generation. *Energy, 29*, 665–676. doi:10.1016/S0360-5442(03)00175-0.

Eck, M., Zarza, E., Eickhoff, M., Rheinlander, J., & Valenzuela, L., 2003. Applied research concerning the direct steam generation in parabolic troughs. *Solar Energy, 74*, 341-351. doi:10.1016/S0038-092X(03)00111-7.

Faccini, J. L., Cunha-Filho, J., De Sampaio, P., & Su, J., 2015. Experimental and Numerical Investigation of Stratified Gas–Liquid Flow in Downward-Inclined Pipes. *Heat Transfer Engineering, 36*(11), 943-951. doi:10.1080/01457632.2015.972729.

Farshi, L., Infante Ferreira, C. A., Mahmoudi, S., & Rosen, M. A., 2014. First and second law analysis of ammonia/salt absorption refrigeration systems. *International Journal of Refrigeration, 40*, 111-121. doi:10.1016/j.ijrefrig.2013.11.006.

Forristal, R., 2003. *Heat Transfer Analysis and Modeling of a Parabolic Trough in Engineering Equation Solver.* Office of Scientific and Technical Information. Oak Ridge: US Department of Energy. Retrieved November 11, 2015, from http://www.ntis.gov/ordering.htm.

Ghoshdastidar, P. S., 2004. *Heat Transfer*, New Delhi, India, Oxford University Press.

Gnielinski, V., 1976. New Equations for heat and Mass Transfer in Turbulent Pipe and Channel Flow Int. *Chemical Engineering, 16*, 359-368.

Haaland, S., 1983. Simple and Explicit Formulas for the Friction Factor in Turbulent Flow. *Journal of Fluids Engineering*, 89–90. doi:10.1115/1.3240948.

Hausen, H., & Düwel, L., 1959. Frage nach dem gleichwertigen Durchmesser bei der Wärmeübertragung in einseitig beheizten Spalten. *Kältetech, 11*, 242-249.

Henning, H., 2007. Solar assisted air conditioning of buildings—an overview. *Applied Thermal Engineering, 27*, 1734–1749. doi:10.1016/j.applthermaleng.2006.07.021.

Hernández-Magallanes, J., Domínguez-Inzunza, L., González-Urueta, G., Soto, P., Jiménez, G., & Rivera, W., 2014. Experimental assessment of an absorption cooling system operating with the ammonia/lithium nitrate mixture. *Energy, 78*, 685-692. Retrieved from http://dx.doi.org/10.1016/j.energy.2014.10.058.

Herold, K., Radermacher, R., & Klein, S., 1996. *Absorption chillers and Heat Pumps.* New York: CRC Press.

Hetsroni, G. e., 1982. *Handbook of Multiphase Systems.* (G. Hetsroni, Ed.) New York, New York, USA: McGraw-Hill.

Infante Ferreira, C., 1984. Thermodynamic and physical property data equations for ammonia-lithium nitrate and ammonia sodium thiocyanate solutions. *Solar Energy, 32*(2), 231–236.

Infante-Ferreira, C., 1985. *Vertical Tubular Absorbers for Ammonia-salt Absorption Refrigeration Ph.D. Thesis.* Delft, The Netherlands: Laboratory for Refrigeration and Indoor Climate Technology, University of Delft. Retrieved August 27, 2016, from uuid:2118f67a-c5ea-4aa3-af23-45e679908eff.

ISO/DIS 9806., 2016. *Solar energy. Solar thermal collectors. Test methods.* ISO. Retrieved August 25, 2016, from http://www.iso.org/iso/catalogue_detail.htm?csnumber=67978.

Issa, R., 1988. Prediction of turbulent, stratified, two-phase flow in inclined pipes and channels. *International Journal of Multiphase Flow, 14*(2), 141-154.

Jradi, M., & Riffat, S., 2012, October. Medium temperature concentrators or solar thermal applications. *International Journal of Low-Carbon Technologies, 0*, 1-11. doi:10.1093/ijlct/cts068.

Kalogirou, S., 2004. Solar thermal collectors and applications. *Progress in Energy and Combustion Science, 30*, 231–295. doi:10.1016/j.pecs.2004.02.001.

Kalogirou, S., Lloyd, S., & Ward, J., 1997. Modelling, optimisation and performance evaluation of a parabolic trough solar collector steam generation system. *Solar Energy, 60*(1), 49-59. doi:10.1016/S0038-092X(96)00131-4.

Kretzschmar, H., Stoecker, I., Kunick, M., & Blaeser, A., 2015, November 5. Property Library for Ammonia. FluiMAT. Zittau, Görlitz, Germany. Retrieved from www.thermodynamics-zittau.de.

Lecuona, A., Ventas, R., Venegas, M., Zacarías, A., & Salgado, R., 2009. Optimum hot water temperature for absorption solar cooling. *Applied Energy, 83*(10), 1806–1814. doi:10.1016/j.solener.2009.06.016.

Lecuona-Neumann, A., Rosner, M., & Ventas-Garzón, R., 2016. Transversal temperature profiles of two-phase stratified flow in the receiver tube of a solar linear concentrator. Simplified analysis. *EUROSON 2016* (p. in press. Palma de Mallorca: ISES.

Libotean, S., Martín, A., Salavera, D., Valles, M., Esteve, X., & Coronas, A., 2008. Densities, Viscosities, and Heat Capacities of AmmoniLithium Nitrate and Ammonia + Lithium Nitrate + Water Solutions between (293.15 and 353.15) K. *Journal of Chemical Engineering Data, 53*(10), 2383–2388. doi:10.1021/je8003035.

Libotean, S., Salavera, D., Valles, M., Esteve, X., & Coronas, A., 2007. Vapor−Liquid Equilibrium of Ammonia + Lithium Nitrate + Water and Ammonia + Lithium Nitrate Solutions from (293.15 to 353.15) K. *Journal of Chemical Engineering Data, 52*(3), 1050–1055. doi:10.1021/je7000045.

Mauthner, F., & Weiss, W., 2013. *Solar Heat Worldwide. Markets and Contribution to the Energy Supply 2011.* International Energy Agency. Paris: International Energy Agency. Solar Heating and Cooling Programm.

Roldán, M., Valenzuela, L., & Zarza, E., 2013. Thermal analysis of solar receiver pipes with superheated steam. *Applied Energy, 103*, 73–84. doi:/10.1016/j.apenergy.2012.10.021.

Sigalés, B., 2003. *Transferencia de Calor Técnica* (Vol. I). Barcelona, Barcelona, Spain: Reverté.

Solar Rating & Certification Corp., 2014. *Certification #10001821 SRCC Standard 600-2013-01 in accordance with EN12975.* Cocoa: Solar Rating & Certification Corporation. Retrieved November 11, 2015, from www.solar-rating.org.

Taitel, Y., & Dukler, A., 1976. A model for predicting flow regime transitions in horizontal and near horizontal gas-liquid flow. *AIChE, 22*, 47-55.

The Carbon Thrust., 2013. *Small-scale Concentrated Solar Power. A review of current activity and potential to accelerate deployment.* London: The Carbon Thrust.

The European Technology Platform on Renewable Heating and Cooling., 2014. *Solar Heating and Cooling. Technology Roadmap.* Brussels. Retrieved November 11, 2015, from www.rhc-platform.org.

Tillner–Roth, R., Harms–Watzenberg, F., & Baehr, H., 1993. Eine neue fundamentalgleichung für Ammoniak. *20th DKV–Tagungsbericht Heidelberg, II*, 167-185.

Turgut, O., Coban, M., & Asker, M., 2016. Comparison of Flow Boiling Pressure Drop Correlations for Smooth Macro tubes. *Heat Transfer Engineering, 37*(6), 487-506. doi:10.1080/01457632.2015.1060733.

Ullmann, A., & Brauner, N., 2006. Closure relations for two-fluid models for two-phase stratified smooth and stratified wavy flows. *International Journal of Multiphase Flow, 32*(1), 82–105. doi:10.1016/j.ijmultiphaseflow.2005.08.005.

Ullmann, A., Goldstein, A., Zamir, M., & Brauner, N., 2004. Closure relations for the shear stresses in two-fluid models for laminar stratified flow. *International Journal of Multiphase Flow, 30*, 877-900. doi:10.1016/j.ijmultiphaseflow.2004.03.008.

Ventas, R., Lecuona, A., Vereda, C., & Legrand, M., 2016. Two-stage double-effect ammonia/lithium nitrate absorption cycle. *Applied Thermal Engineering, 94*, 228–237. Retrieved from http://dx.doi.org/10.1016/j.applthermaleng.2015.10.144.

Ventas, R., Lecuona, A., Zacarías, A., & Venegas, M., 2010. Ammonia-Lithium Nitrate Absorption Chiller With An Integrated Low-Pressure Compression Booster Cycle For Low Driving Temperatures. *Applied Thermal Engineering, 30*, Volume 30, Iss1351-1359. doi:10.1016/j.applthermaleng.2010.02.022.

Vereda, C., Ventas, R., Lecuona, A., & López, R., 2014. Single-effect absorption refrigeration cycle boosted with an ejector-adiabatic absorber using a single solution pump. *International Journal of Refrigeration, 38*, 22-29. doi:10.1016/j.irefrig.2013.10.010.

Wallis, G., 1969. *One-Dimensional Two-phase Flow.* New York: McGraw-Hill Book Co.

Wang, F., Feng, H., Zhao, J., Li, W., Zhang, F., & Liu, R., 2015. Performance assessment of solar assisted absorption heat pump system with parabolic trough collectors. *Energy Procedia, 70*, 529 – 536. doi:10.1016/j.egypro.2015.02.157.

Wu, W., Wang, B., Shi, W., & Li, X., 2013. Crystallization Analysis and Control of Ammonia-Based Air Source Absorption Heat Pump in Cold Regions. *Advances in Mechanical Engineering, 5*, 140341. doi:10.1155/2013/140341.

Wu, W., Wang, B., Shi, W., & Li, X., 2014. An overview of ammonia-based absorption chillers and heat pumps. *Renewable and Sustainable Energy Reviews, 31*, 681–707. doi:http://dx.doi.org/10.1016/j.rser.2013.12.021.

Yu, N., Wang, R., & Wang, L., 2013. Sorption thermal storage for solar energy. *Progress in Energy and Combustion Science, 39*, 489-514. doi:10.1016/j.pecs.2013.05.004.

Zamora, M., Bourouis, M., Coronas, A., & Vallés, M., 2014. Pre-industrial development and experimental characterization of new air-cooled and water cooled ammonia/lithium nitrate absorption chillers. *International journal of refrigeration, 45*, 189-197. doi:10.1016/j.ijrefrig.2014.06.005.